

# MAVias: Mitigate any Visual Bias

Ioannis Sarridis<sup>1,2</sup> Christos Koutlis<sup>1</sup> Symeon Papadopoulos<sup>1</sup> Christos Diou<sup>2</sup>

<sup>1</sup>Information Technologies Institute, CERTH, Thessaloniki, Greece

<sup>2</sup>Department of Informatics and Telematics, Harokopio University, Athens, Greece

{gsarridis, ckoutlis, papadop}@iti.gr {isarridis, cdiou}@hua.gr

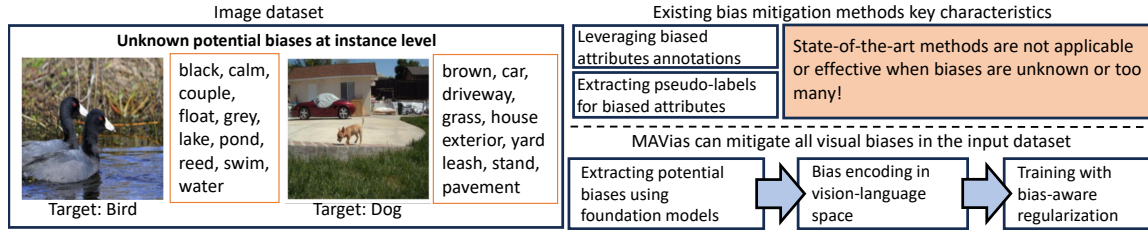


Figure 1. MAVias identifies visual biases through foundational models that extract tags representing visual features and assess relevance to the target class. Then, MAVias encodes these features within the vision-language space and integrates them into a bias-aware framework to train a model that is invariant to such visual biases.

## Abstract

Mitigating biases in computer vision models is an essential step towards the trustworthiness of artificial intelligence models. Existing bias mitigation methods focus on a small set of predefined biases, limiting their applicability in visual datasets where multiple, possibly unknown biases exist. To address this limitation, we introduce MAVias, an open-set bias mitigation approach leveraging foundation models to discover spurious associations between visual attributes and target classes. MAVias first captures a wide variety of visual features in natural language via a foundation image tagging model, and then leverages a large language model to select those visual features defining the target class, resulting in a set of language-coded potential visual biases. We then translate this set of potential biases into vision-language embeddings and introduce an in-processing bias mitigation approach to prevent the model from encoding information re-

lated to them. Our experiments on diverse datasets, including CelebA, Waterbirds, ImageNet, and UrbanCars, show that MAVias effectively detects and mitigates a wide range of biases in visual recognition tasks outperforming current state-of-the-art.

## 1. Introduction

Computer Vision (CV) progress has been largely driven by Deep Learning (DL) advances [9, 15] and large-scale datasets [6, 21, 25], enabling models to learn complex patterns and visual features with impressive accuracy. However, alongside this progress, concerns have emerged about biases embedded in these models [11, 29, 32, 38, 41, 44] – often stemming from unintended correlations present in the training data [13, 22, 27, 30]. The correlated attributes that are irrelevant, act as “shortcuts” and can significantly impact the model’s reliability and generalization [12, 37]. It is important to note

that in the context of this paper, we define as visual bias any characteristic that does not contribute to defining the target class, which we refer to as “irrelevant”. To address this, several methodologies have been developed. Broadly, these fall into two categories: Bias Label-Aware (BLA) and Label-Unaware (BLU) methods. BLA methods leverage the annotations of the attributes introducing the biases to address them [2, 19, 42, 45]. BLU methods focus on extracting bias pseudo-labels in cases of extreme biases where a bias-proxy model (or bias-capturing classifier) can be trained using the task’s target labels that closely align with the bias labels [16, 28, 31, 39].

While effective in certain contexts, both BLA and BLU methods are limited in their applicability when there are multiple, complex, and possibly unknown biases. Common challenging scenarios include:

**Unknown biases.** In large-scale, general-purpose CV datasets, such as ImageNet, biases may be difficult to identify and largely remain unknown, as they vary widely between different classes and are not prominent enough to allow training of a bias proxy model. For instance, in the ImageNet9 example presented in Tab. 1, a sample labeled as a *dog* could introduce biases related to the background scene (e.g., *armchair*, *couch*, *pillow*, *red*), the color of the dog (e.g., *black* and *white*), or accessories like a *neckband*.

**Potential biases beyond a predefined set.** The CelebA example in Tab. 1, shows that beyond the *hair color*, additional biases may be present, such as clothing styles (e.g., *business suit*, *tie*).

**Poor representation of predefined bias.** In some cases, biases are reduced to single labels, such as “rural background” in the UrbanCars dataset. However, as shown in Tab. 1, more nuanced descriptors at the instance level (e.g., *path*, *tree*, *wood*, *forest*, *hydrant*, *red*, etc.) provide a richer context for modeling bias.

Existing BLA and BLU methods are not designed to mitigate such biases, leading to models that are biased and/or do not achieve their optimal generalization potential. To address this, Mitigate Any Visual bias (MAVias) introduces a flexible and

scalable solution, capable of identifying and mitigating open-set biases in CV datasets. MAVias begins by extracting descriptive tags that capture various visual features, such as general-purpose objects, actions, scenes, and visual attributes. Note that a sufficiently large and comprehensive vocabulary can cover the vast majority of visual features present in CV datasets, enabling the method to be considered as operating in an open-set setting. Then, these tags are processed by a Large Language Model (LLM) to identify which ones are irrelevant to each of the target classes, leading to a rich set of *language-encoded visual biases*, text descriptions of visual characteristics that are irrelevant to the classification task at hand. We then translate these biases into vision-language embeddings, project them to the main model’s backbone space and then to the classification layer. This projection layer is trained simultaneously alongside the main model, and during training, the output logits are a linear combination of the logits of the main model and those of the projection layer that capture visual biases. This setup allows the main model to be exposed to the biased features – those representing irrelevant information to the target class – in a controlled way that leads to bias-invariant representations. Overall, MAVias provides an effective, end-to-end solution for identifying and mitigating biases in open-set scenarios. We evaluate the proposed method on several datasets involving single-attribute biases (CelebA, Waterbirds) as well as multi-attribute predefined biases (UrbanCars) demonstrating state-of-the-art performance. Furthermore, experiments were conducted on ImageNet9, involving unknown biases, where the suggested approach demonstrates significant gains (from 5.24% to 10.21%) in terms of accuracy compared to existing competitive approaches.

The main contributions of this paper are the following: (i) a framework for identifying instance-specific open-set potential visual biases in CV datasets, (ii) a learning strategy that exploits foundation models to learn bias-invariant representations, and (iii) an extensive evaluation study including comparative and ablation experiments across 4 thematically diverse datasets demonstrating the

effectiveness and general applicability of the proposed method, which outperforms the current state-of-the-art.

## 2. Related Work

**Bias identification** Several methods recently emerged that leverage text (such as captions, keywords, or tags) for bias detection, highlighting the potential of this approach in this domain. For instance, Say My Name (SaMyNa) [4] is an explainability method that tries to discover model biases through text-based pipelines. Similarly, the Bias-to-Text (B2T) [20] and Language-guided (Lg) [50] frameworks discover biases by extracting common keywords from the captions of misclassified images. These methods aim to identify the main source of bias (e.g., *hair color* in the CelebA example illustrated in Fig. 1) rather than discovering any potentially biased visual characteristic in an open-set setting. Furthermore, OpenBias [8] introduces a framework for detecting biases in text-to-image generative models by leveraging LLMs to propose potential biases from captions. Although operating in a different domain (text-to-image generation), similarly to MAVias OpenBias acknowledges the need for discovering potential biases in an open-set setting. However, it solely relies on an LLM to generate specific bias lists for a given caption, raising concerns about whether the LLM’s interpretation of biases aligns with human judgment. In contrast, MAVias takes a more structured and systematic approach; it evaluates each descriptive tag by querying the LLM to determine whether it is directly relevant to the target class using a detailed prompt (refer to the Appendix for system prompt details).

**Bias mitigation** Recent efforts to mitigate bias in CV have led to the development of various methodologies, including methods with direct access to the labels of attributes introducing bias (i.e., BLA methods) [2, 16, 19, 24, 35, 37, 42, 45] and methods that do not take advantage of such labels but instead rely on deriving pseudo-labels (i.e., BLU methods) [1, 3, 31, 39, 46]. For instance, Learn-

ing Not to Learn (LNL) [19] is a BLA method that discourages the model from predicting the attribute introducing bias, while Bias Contrastive-Bias Balance (BC-BB) [16] and FairKL [2] rely on the bias labels to enforce bias-neutral pairwise similarities between the samples using contrastive learning. Some methods have indirect access to the bias labels by utilizing bias-capturing classifiers trained on different datasets offering bias-related information explicitly [39, 40]. Finally, other methods infer pseudo-labels from the biased vanilla model to identify the biases [1, 5, 31]. While these methods have been effective in mitigating biases, they primarily depend on predefined bias labels or pseudo-labels derived from biased models. On the contrary, this work investigates open-set scenarios and introduces a flexible bias mitigation methodology that can discover and handle multiple, diverse biases without requiring a unified bias-labeling system across all the dataset’s samples.

## 3. Methodology

### 3.1. Problem Formulation

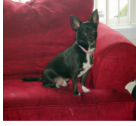



Let  $\mathcal{D} = \{(\mathbf{x}^{(i)}, y^{(i)})\}_{i=1}^N$  be a dataset consisting of  $N$  images, where  $\mathbf{x}^{(i)} \in \mathcal{X}$  represents an input image, and  $y^{(i)} \in \mathcal{Y}$  is the corresponding target label. The goal is to train a DL model  $f_{\theta} : \mathcal{X} \rightarrow \mathcal{Y}$ , parameterized by  $\theta$ , to predict the target label  $y^{(i)}$  given an image  $\mathbf{x}^{(i)}$ , while mitigating a set of potential biases,  $\mathcal{B}^{(i)}$ , present in  $\mathbf{x}^{(i)}$  that may lead to biased predictions. In this context the term “potential biases” refers to all visual attributes present in  $\mathcal{X}$  that are irrelevant to the target class, such as elements of the background of images.

### 3.2. Methodology

#### 3.2.1. Language-driven Bias Modeling

First, MAVias utilizes an image tagging model to extract descriptive tags that represent the visual information present in an image. In many general-purpose CV datasets, biases consist of visual information that can be described in text. Formally, for each image  $\mathbf{x}^{(i)}$ , we derive a set of tags  $\mathcal{T}^{(i)} = \{t_1^{(i)}, t_2^{(i)}, \dots, t_m^{(i)}\}$ , where  $m$  represents the total number of tags. These capture various visual at-

Table 1. Examples of extracted tags for various datasets. Red color indicates the irrelevant tags ( $\mathcal{B}^{(i)}$ ).

Dataset	ImageNet9	Waterbirds	UrbanCars	CelebA
Target Class	dog	bird species	car type	gender
Bias Type	unknown	background	background and objects	hair colour
Sample				
Extracted Tags	armchair, black, chair, couch, dog, neckband, pillow, red, sit, white,	bamboo, bamboo forest, bird, blue, branch, green, hide, parrot, perch, sit, stand, stem, tree, yellow,	car, path, forest, hydrant, lush, park, red, road, sedan, silver, SUV, tree, white, wood,	black, business suit, dress, dress shirt, man, stand, stare, suit, tie, wear,

tributes, including colors, objects, backgrounds, and other features that can either describe the target class or introduce bias.

The next step is to filter out tags that should not influence the decisions of a robust classifier. To achieve this, we leverage an LLM to identify which tags are irrelevant to the target class  $y^{(i)}$ . We denote this subset of potential biases as  $\mathcal{B}^{(i)} \subseteq \mathcal{T}^{(i)}$ . These encapsulate visual features that could lead to biased predictions if considered by the model. To ensure the LLM correctly identifies these irrelevant tags, we carefully design the prompt used for this task by providing precise instructions on what tag should be considered relevant (e.g., physical components, defining features, inherent characteristics, etc.) or not (e.g., background details, lighting, textures, other objects, etc.). Details on the prompt formulation process are provided in the Appendix. Table 1 shows several examples of  $\mathcal{B}^{(i)}$  for samples belonging to different datasets.

For each set of irrelevant tags  $\mathcal{B}^{(i)}$  associated with an image  $\mathbf{x}^{(i)}$ , we employ a vision-language model to generate a single embedding  $\mathbf{e}^{(i)} \in \mathbb{R}^d$ , where  $d$  is the dimension of the embedding. This is produced using the prompt “a photo of  $t_1^{(i)}, t_2^{(i)}, \dots, t_k^{(i)}$ ”, where  $k \leq m$  is the number of irrelevant tags. This aggregate embedding captures the combined information from all irrelevant tags, providing an instance-level representation of the biased features that could affect the model’s be-

havior. Comparison with alternative embedding approaches is provided in Appendix.

### 3.2.2. Bias Mitigation

We define the main model  $f_{\theta}(\mathbf{x}^{(i)})$ , a DL classifier composed of the following: (i) a backbone  $f_{\theta_{bb}}(\mathbf{x}^{(i)})$ , which extracts feature representations  $\mathbf{h}^{(i)} \in \mathbb{R}^r$ , where  $r$  is the feature vector size; (ii) a classification head  $f_{\theta_c}(\mathbf{x}^{(i)})$  outputting the logits  $\mathbf{z}_{\text{main}}^{(i)} = f_{\theta_c}(\mathbf{h}^{(i)}) \in \mathbb{R}^p$ , where  $p$  is the number of classes. Thus, the overall main model is expressed as:

$$f_{\theta}(\mathbf{x}^{(i)}) = f_{\theta_c}(f_{\theta_{bb}}(\mathbf{x}^{(i)})). \quad (1)$$

In parallel, we introduce a projection layer  $g_{\phi}$ , parameterized by  $\phi$ , which takes the visual bias embeddings  $\mathbf{e}^{(i)}$  as input and outputs embeddings  $\mathbf{b}^{(i)} \in \mathbb{R}^p$ . Note that  $g_{\phi}$  is employed to project  $\mathbf{e}^{(i)}$  to the feature space of  $\mathbf{h}^{(i)}$ . Then the corresponding logits are derived through  $\mathbf{z}_{\text{tag}}^{(i)} = f_{\theta_c}(\mathbf{b}^{(i)}) \in \mathbb{R}^p$ . The final logits  $\mathbf{z}^{(i)}$  for each sample are the addition of the main model logits  $\mathbf{z}_{\text{main}}^{(i)}$  and the visual bias logits  $\mathbf{z}_{\text{tag}}^{(i)}$ :

$$\mathbf{z}^{(i)} = \mathbf{z}_{\text{main}}^{(i)} + \mathbf{z}_{\text{tag}}^{(i)}. \quad (2)$$

It is worth noting that bias often arises during DL model training because biased attributes in the training data are easier to learn and thus dominate gradient updates [34]. To counteract this, MAVias incorporates visual bias logits into the

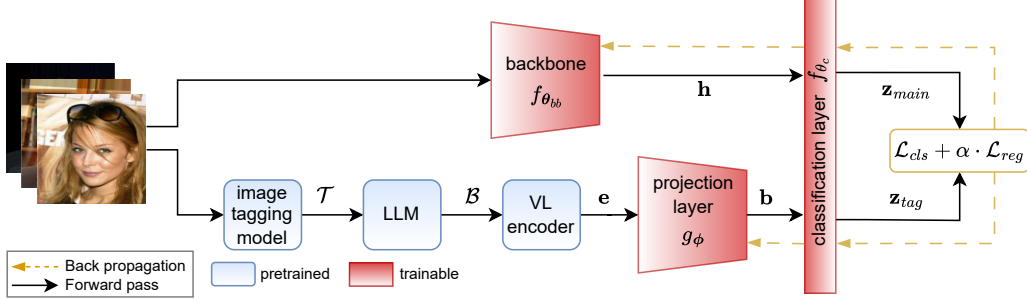


Figure 2. Illustration of the proposed framework for mitigating any visual bias during model training. For inference, only the backbone and the classification layer are considered (i.e.,  $f_{\theta}$ ).

main model’s logits, ensuring that as the bias in a sample increases, its impact on gradient updates is reduced. The intuition behind this mechanism is that for bias-aligned samples, the value of  $\mathbf{z}_{tag}$  is high, effectively reducing the magnitude of  $\mathbf{z}_{main}$  and its contribution to the total logits  $\mathbf{z}$ . This leads to significantly reduced gradients for these samples. This is supported both empirically in Sec. 4.2 and theoretically in the Appendix. In other words,  $\mathbf{z}_{tag}$  assists in decoupling the learning of biased features from the actual task at hand, which allows the main model to focus on the relevant features for the target prediction.

Furthermore, since both the main model and the projection layer are trained concurrently, it is essential to ensure the stability of the training process. To achieve this, we introduce a loss function that combines the classification loss with a regularization term. The classification loss ensures that the combined logits  $\mathbf{z}^{(i)}$  accurately predict the target label  $y^{(i)}$ , while the regularization term aligns the magnitude of the main model’s logits  $\mathbf{z}_{main}^{(i)}$  with those of the visual bias logits  $\mathbf{z}_{tag}^{(i)}$ . By doing so, we prevent  $g_{\phi}$  from dominating or being overshadowed by  $h_{\theta}$ .

Specifically, the total loss is computed as:

$$\mathcal{L}(\theta, \phi) = \mathcal{L}_{cls}(\mathbf{z}^{(i)}, y^{(i)}) + \alpha \cdot \mathcal{L}_{reg}(\mathbf{z}_{main}^{(i)}, \mathbf{z}_{tag}^{(i)})$$

where: (i)  $\mathcal{L}_{cls}(\mathbf{z}^{(i)}, y^{(i)})$  is the classification loss (e.g., cross-entropy loss) between the final

logits  $\mathbf{z}^{(i)}$  and the ground truth label  $y^{(i)}$ ; (ii)  $\mathcal{L}_{reg}(\mathbf{z}_{main}^{(i)}, \mathbf{z}_{tag}^{(i)})$  is the regularization term for the norm of the logits, calculated as:

$$\mathcal{L}_{reg}^{(i)} = \frac{1}{2} \left\| \|\mathbf{z}_{main}^{(i)}\| - \lambda \cdot \|\mathbf{z}_{tag}^{(i)}\| \right\|^2 \quad (3)$$

where  $\|\cdot\|$  denotes the  $l^2$ -norm,  $\lambda \in (0, 1)$  is a scaling factor and  $\alpha \in (0, 1)$  is a weighting factor that balances the influence of the  $\mathcal{L}_{reg}(\mathbf{z}_{main}^{(i)}, \mathbf{z}_{tag}^{(i)})$  in the total loss function. Typically, the greater the bias in the data, the smaller the value of  $\lambda$  should be, as this leads to smaller  $\mathbf{z}_{main}$  values and reduced gradient updates for the bias-aligned samples. Further details on the effects of hyperparameters  $\lambda$  and  $\alpha$  are provided in the Appendix. The overview of the proposed framework is illustrated in Fig. 2.

## 4. Experiments

### 4.1. Datasets and Evaluation Protocol

We employ Biased-CelebA [16], Waterbirds [37], UrbanCars [24], and Imagenet9 [47]. Biased-CelebA is a subset of the well-known CelebA dataset consisting of facial images annotated with 40 binary attributes. In this subset, *gender* is treated as the target attribute, while the *BlondHair* attribute introduces bias by enforcing a 90% correlation between the two. Waterbirds is a dataset that features a co-occurrence of 95% between waterbirds (or landbirds) and aquatic environments (or terrestrial environments) as background. UrbanCars is



an artificially generated dataset featuring a 95% co-occurrence between car body types and background and/or certain objects relevant to urban or rural regions. ImageNet9 consists of 9 coarse ImageNet classes (dog, bird, vehicle, reptile, carnivore, insect, instrument, primate, and fish).

Regarding the evaluation, we follow the protocols suggested by the dataset providers and previous works. In particular, for CelebA we use the accuracy of the underrepresented groups (i.e., bias-conflicting accuracy) and the average accuracy across all groups (i.e., unbiased accuracy) [16, 39]. For Waterbirds, we use the Worst-Group (WG) accuracy and the average accuracy across all groups. In the case of UrbanCars, we calculate the weighted average accuracy across groups, referred to as In-Distribution Accuracy (I.D. Acc), with weights determined by group representation ratios. Furthermore, I.D. Acc serves as a baseline for assessing accuracy drops related to background (BG Gap), co-occurring objects (CoObj Gap), and both background and co-occurring objects combined (BG+CoObj Gap). Lastly, for ImageNet9, we use 7 test set variations for evaluating the impact of background on model’s predictions: ORIGINAL, ONLY-BG-B (black object’s bounding box), ONLY-BG-T (impainted object’s bounding box), NO-FG Black (removed segmented object), ONLY-FG (black background), MIXED-RAND (random background of a random class), and MIXED-NEXT (random background of the next class).

## 4.2. Comparative analysis

In this subsection, we compare the performance of MAVias with other competitive BLU methods. Comprehensive results, including comparisons with BLA methods, are provided in the Appendix. Table 2 presents the performance of MAVias on CelebA with *gender* as target and the *BlondHair* as the biased attribute. The performance on unbiased and bias-conflicting samples indicates the ability of MAVias to reduce reliance on spurious correlations between the target and the corresponding biased attributes. Specifically, MAVias achieves 87.1% accuracy on bias-conflicting sam-

Table 2. Evaluation on CelebA with *BlondHair* and *gender* as biased attribute and target, respectively.

Methods	Unbiased	Bias-conflict
LfF [31]	84.2±0.3	81.2±1.4
SoftCon [16]	84.1	74.4
FLAC-B [39]	87.0±0.6	84.9±2.2
MAVias	<b>89.7±0.6</b>	<b>87.1±1.7</b>

Table 3. Evaluation on Waterbirds.

Method	WG Acc.	Avg. Acc.
JTT [26]	86.7±1.5	93.3±0.3
DISC [46]	88.7±0.4	93.8±0.7
MAVias	<b>93.7±0.4</b>	<b>94.5±0.4</b>

Table 4. Evaluation on UrbanCars.

Method	I.D. Acc	BG Gap	CoObj Gap	BG+CoObj Gap
LfF [31]	97.2	-11.6	-18.4	-63.2
JTT [26]	95.9	-8.1	-13.3	-40.1
Debian [23]	98.0	-14.9	-10.5	-69.0
MAVias	92.8±0.8	<b>-4.1±0.6</b>	<b>-2.4±1.4</b>	<b>-6.7±1.4</b>

ples, surpassing state-of-the-art BLU methods such as FLAC-B [39] and LfF [31], while maintaining high unbiased accuracy (89.7%).

Table 3 evaluates MAVias on Waterbirds, a well-known benchmark for spurious correlation problems between bird type and background environment. Notably, MAVias attains 93.7% Worst-Group accuracy, outperforming all compared BLU methods (+5%), while slightly improving the average accuracy (+0.7%). The results on UrbanCars in Tab. 4 further validate the efficacy of MAVias in mitigating multiple biases introduced by co-occurring objects and background features. While the in-distribution accuracy (I.D. Acc) of MAVias is marginally lower than that of LfF [31] or Debian [23], it achieves substantial improvements in reducing the BG Gap (-4.1) and CoObj Gap (-2.4), as well as their combined effects (BG+CoObj Gap: -6.7).

In addition, we examine the logit space of the models to demonstrate the effect of MAVias on the behavior of the main model. Similar to the pre-

Table 5. Accuracy on ImageNet9 test sets. The reported results for the compared methods are based on reimplementations using code provided by the authors of [24].

Method	MIXED-NEXT ( $\uparrow$ )	MIXED-RAND ( $\uparrow$ )	NO-FG ( $\downarrow$ )	ONLY-BG-B ( $\downarrow$ )	ONLY-BG-T ( $\downarrow$ )	ONLY-FG ( $\uparrow$ )	ORIGINAL ( $\uparrow$ )
Vanilla	82.66 $\pm$ 0.1	85.06 $\pm$ 0.0	64.16 $\pm$ 0.1	35.18 $\pm$ 0.1	44.74 $\pm$ 0.1	<b>93.12</b> $\pm$ 0.0	97.69 $\pm$ 0.0
LfF [31]	78.70 $\pm$ 0.1	81.47 $\pm$ 0.2	61.07 $\pm$ 0.1	34.82 $\pm$ 0.2	44.46 $\pm$ 0.0	88.99 $\pm$ 0.2	94.34 $\pm$ 0.2
JTT [26]	84.43 $\pm$ 0.1	86.16 $\pm$ 0.5	61.09 $\pm$ 0.2	32.04 $\pm$ 1.0	36.62 $\pm$ 4.7	92.09 $\pm$ 0.5	97.71 $\pm$ 0.1
Debian [23]	83.02 $\pm$ 0.4	85.64 $\pm$ 0.3	64.53 $\pm$ 0.4	34.45 $\pm$ 0.1	45.00 $\pm$ 0.6	93.06 $\pm$ 0.1	<b>97.89</b> $\pm$ 0.1
MAViAs	<b>88.26</b> $\pm$ 0.1 (+5.24)	<b>89.64</b> $\pm$ 0.2 (+3.48)	<b>53.02</b> $\pm$ 0.7 (+8.05)	<b>21.83</b> $\pm$ 0.4 (-10.21)	<b>32.48</b> $\pm$ 0.6 (-4.14)	91.90 $\pm$ 0.4 (-1.22)	96.92 $\pm$ 0.2 (-0.97)

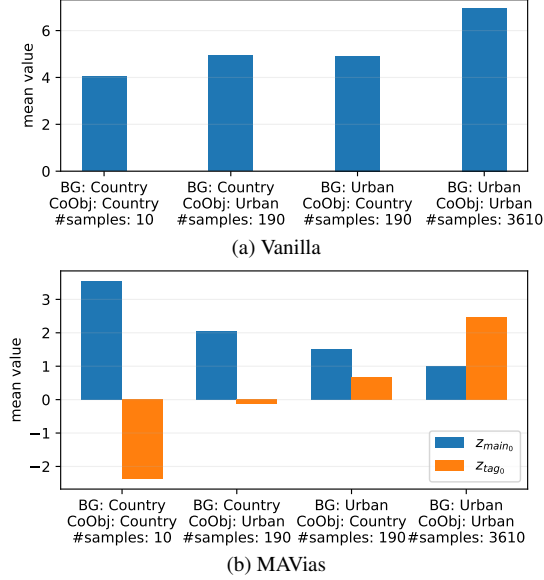


Figure 3. Logits for UrbanCars training samples belonging to groups defined by the *urban car* class and Background (BG) and Co-occurring Object (CoObj) biases.

vious experiment, the *urban car* class of the UrbanCars dataset is used. As one may observe in Fig. 3 (a), the vanilla (biased) model increases the logit values proportionally with the bias, ranging from 4 to 7. This is an expected behavior, as the biases (i.e., spurious correlations) are easier to learn than the actual target and thus the model illustrates higher confidence (or logit values) for the bias-aligned samples. This phenomenon is referred to as Gradient Starvation [34] and can describe how bias is introduced to the models. Also, it is theoretically shown that methodologies penalizing high logit values can mitigate this phenomenon [34]. As shown in Fig. 3 (b), the interactions between the

main model and the projection layer in the training procedure (defined by Eq. s (2) and (3)) successfully reduce the main model’s logits values proportionally to the bias in the data.

Apart from the typical training datasets designed for BLA methods, we also consider experiments on ImageNet9, a widely used CV dataset known for various tasks and equipped with multiple test sets specifically designed for bias evaluation. As shown in Tab. 5, MAViAs achieves great improvements in the model’s accuracy on the test sets with modified backgrounds (i.e., MIXED-NEXT and MIXED-RAND), with the highest gains occurring for the MIXED-NEXT set (+5.24%) compared to the second best performing method. Similarly, for the sets where background information is suppressed (ONLY-BG-B, ONLY-BG-T, and NO-FG) MAViAs achieves improvements of +10.21%, +4.14%, and +8.05%, respectively. As observed, all competitive methods, including MAViAs, demonstrate reduced performance on ONLY-FG compared to the vanilla model. This is likely because the vanilla model can exploit biases present in the foreground (e.g., colors) to increase its accuracy. Finally, there is a 0.97% drop in performance on the ORIGINAL test set, which aligns with expectations, as MAViAs is designed to rely less on shortcuts that boost overall performance. Furthermore, we evaluate MAViAs using two subsets of ImageNet9 ORIGINAL, constructed based on tags identified by MAViAs. Specifically, the *bias-aligned* set includes samples with tags for which the vanilla model performs above its overall accuracy, suggesting high bias impact; the rest of the samples form the *bias-conflicting* set. Table 6 demonstrates that MAViAs improves accuracy on bias-conflicting samples by reducing reliance on visual biases, with a slight de-

Table 6. Evaluation on the ImageNet9 ORIGINAL set comparing accuracy on the samples with irrelevant tags for which the Vanilla model overperforms (bias-aligned, BA) and the rest of the samples (bias-conflicting, BC).

Method	BA acc.	BC acc.	Gap
Vanilla	98.55 $\pm$ 0.04	90.86 $\pm$ 0.11	-7.69 $\pm$ 0.16
MAVias	97.3 $\pm$ 0.21	94.13 $\pm$ 0.01	<b>-3.17</b> $\pm$ 0.21

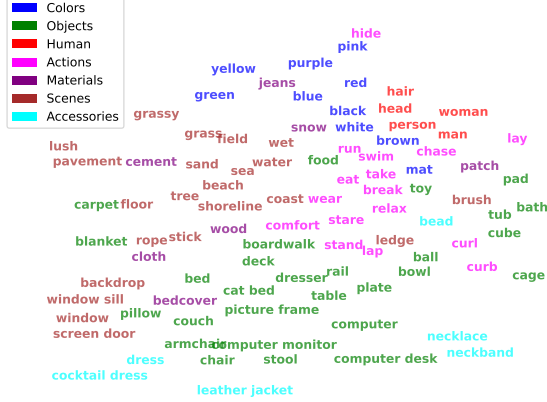


Figure 4. Visualization of the biases identified using MAVias for the Dog class in the ImageNet9 dataset.

crease on bias-aligned samples for the same reason. Finally, to gain a clearer understanding, Fig. 4 visualizes the bias-aligned tags for the Dog class in the bias-aligned set.

### 4.3. Ablation Analysis

An important aspect in MAVias is how the embeddings are calculated. Table 7 compares two well-known vision-language models, i.e., CLIP and SigLip, and the text-based model BERT. Further-

Table 7. Impact of the employed encoders on the MAVias performance. Results pertain to the Waterbirds dataset.

Model	WG Acc.	Avg. Acc.
BERT [7]	91.7 $\pm$ 1.3	92.8 $\pm$ 1.0
SigLip [48]	92.7 $\pm$ 1.2	93.5 $\pm$ 1.0
CLIP [36]	93.7 $\pm$ 0.4	94.5 $\pm$ 0.4

more, Tab. 8 compares MAVias’s performance using various LLMs. ChatGPT-4o shows the high-

Table 8. Impact of the employed LLM on the MAVias performance. Results pertain to the Waterbirds dataset.

Model	#parameters	WG Acc.	Avg. Acc.
Qwen2.5 [17]	7b	91.9 $\pm$ 2.4	94.4 $\pm$ 0.5
Mistral-small [18]	22b	92.9 $\pm$ 0.4	94.9 $\pm$ 0.2
Gemma2 [43]	9b	93.5 $\pm$ 0.6	94.5 $\pm$ 0.6
Llama3.1 [10]	8b	93.6 $\pm$ 0.6	94.4 $\pm$ 0.4
ChatGPT-4o [33]	>>175b	93.7 $\pm$ 0.4	94.5 $\pm$ 0.4

Table 9. Impact of Eq. (3) on the MAVias performance. Results pertain to Waterbirds dataset.

Type	WG Acc.	Avg. Acc.
w/o regularizer	89.4 $\pm$ 1.6	95.2 $\pm$ 0.4
w/ regularizer	93.7 $\pm$ 0.4	94.5 $\pm$ 0.4

est performance, with open-source models also performing competitively. For experiments, we use ChatGPT-4o to minimize LLM-related errors. Finally, as discussed in Sec. 3, the regularization term in Eq. (3) is crucial for balancing the logits between the two models. Table 9 shows the impact of removing this term from the training on the effectiveness of MAVias. Note that in the Appendix, we also investigate different methods for computing embeddings from tags and examine the effect of the tags’ vocabulary size.

## 5. Conclusion

In this work, we presented a framework to address open-set biases in CV using instance-level descriptive tags. Unlike traditional methods relying on predefined biases, MAVias offers a flexible, scalable solution for identifying and mitigating unknown biases. It detects visual features that may introduce bias and reduces their impact through a robust approach. Extensive experiments show MAVias outperforms existing methods in detecting and mitigating complex, real-world biases. The main requirement is an image tagging model with a comprehensive tag vocabulary and an LLM suited to the data context. For example, cloud-deployed models are not ideal for sensitive data like medical images.



## References

- [1] Hyojin Bahng, Sanghyuk Chun, Sangdoo Yun, Jaegul Choo, and Seong Joon Oh. Learning de-biased representations with biased representations. In *International Conference on Machine Learning*, pages 528–539. PMLR, 2020. 3
- [2] Carlo Alberto Barbano, Benoit Dufumier, Enzo Tartaglione, Marco Grangetto, and Pietro Gori. Unbiased supervised contrastive learning. *arXiv preprint arXiv:2211.05568*, 2022. 2, 3, 13, 15
- [3] Remi Cadene, Corentin Dancette, Matthieu Cord, Devi Parikh, et al. Rubi: Reducing unimodal biases for visual question answering. *Advances in neural information processing systems*, 32, 2019. 3
- [4] Massimiliano Ciranni, Luca Molinaro, Carlo Alberto Barbano, Attilio Fiandrotti, Vittorio Murino, Vito Paolo Pastore, and Enzo Tartaglione. Say my name: a model’s bias discovery framework. *arXiv preprint arXiv:2408.09570*, 2024. 3
- [5] Christopher Clark, Mark Yatskar, and Luke Zettlemoyer. Don’t take the easy way out: Ensemble based methods for avoiding known dataset biases. In *Proceedings of the 2019 Conference on Empirical Methods in Natural Language Processing and the 9th International Joint Conference on Natural Language Processing (EMNLP-IJCNLP)*, pages 4069–4082, 2019. 3
- [6] Jia Deng, Wei Dong, Richard Socher, Li-Jia Li, Kai Li, and Li Fei-Fei. Imagenet: A large-scale hierarchical image database. In *2009 IEEE Conference on Computer Vision and Pattern Recognition*, pages 248–255. IEEE, 2009. 1
- [7] Jacob Devlin, Ming-Wei Chang, Kenton Lee, and Kristina Toutanova. BERT: pre-training of deep bidirectional transformers for language understanding. In *Proceedings of the 2019 Conference of the North American Chapter of the Association for Computational Linguistics: Human Language Technologies, NAACL-HLT 2019, Minneapolis, MN, USA, June 2-7, 2019, Volume 1 (Long and Short Papers)*, pages 4171–4186. Association for Computational Linguistics, 2019. 8
- [8] Moreno D’Incà, Elia Peruzzo, Massimiliano Mancini, Dejie Xu, Vidit Goel, Xingqian Xu, Zhangyang Wang, Humphrey Shi, and Nicu Sebe. Openbias: Open-set bias detection in text-to-image generative models. In *Proceedings of the IEEE/CVF Conference on Computer Vision and Pattern Recognition*, pages 12225–12235, 2024. 3
- [9] Alexey Dosovitskiy. An image is worth 16x16 words: Transformers for image recognition at scale. *arXiv preprint arXiv:2010.11929*, 2020. 1
- [10] Abhimanyu Dubey, Abhinav Jauhri, Abhinav Pandey, Abhishek Kadian, Ahmad Al-Dahle, Aiesha Letman, Akhil Mathur, Alan Schelten, Amy Yang, Angela Fan, et al. The llama 3 herd of models. *arXiv preprint arXiv:2407.21783*, 2024. 8
- [11] Simone Fabbrizzi, Symeon Papadopoulos, Eirini Ntoutsi, and Ioannis Kompatsiaris. A survey on bias in visual datasets. *Computer Vision and Image Understanding*, 223:103552, 2022. 1
- [12] Abhinav Gupta, Adithyavairavan Murali, Dhiraaj Prakashchand Gandhi, and Lerrel Pinto. Robot learning in homes: Improving generalization and reducing dataset bias. *Advances in neural information processing systems*, 31, 2018. 1
- [13] Shashank Gupta, Vaishnavi Shrivastava, Ameet Deshpande, Ashwin Kalyan, Peter Clark, Ashish Sabharwal, and Tushar Khot. Bias runs deep: Implicit reasoning biases in persona-assigned LLMs. In *The Twelfth International Conference on Learning Representations*, 2024. 1
- [14] Kaiming He, Xiangyu Zhang, Shaoqing Ren, and Jian Sun. Deep residual learning for image recognition. In *Proceedings of the IEEE conference on computer vision and pattern recognition*, pages 770–778, 2016. 13
- [15] Jonathan Ho, Ajay Jain, and Pieter Abbeel. Denoising diffusion probabilistic models. *Advances in neural information processing systems*, 33:6840–6851, 2020. 1
- [16] Youngkyu Hong and Eunho Yang. Unbiased classification through bias-contrastive and bias-balanced learning. *Advances in Neural Information Processing Systems*, 34:26449–26461, 2021. 2, 3, 5, 6, 12, 13, 15
- [17] Binyuan Hui, Jian Yang, Zeyu Cui, Jiaxi Yang, Dayiheng Liu, Lei Zhang, Tianyu Liu, Jiajun Zhang, Bowen Yu, Kai Dang, et al. Qwen2. 5-coder technical report. *arXiv preprint arXiv:2409.12186*, 2024. 8
- [18] Albert Q Jiang, Alexandre Sablayrolles, Arthur Mensch, Chris Bamford, Devendra Singh Chaplot, Diego de las Casas, Florian Bressand, Gianna Lengyel, Guillaume Lample, Lucile Saulnier, et al. Mistral 7b. *arXiv preprint arXiv:2310.06825*, 2023. 8
- [19] Byungju Kim, Hyunwoo Kim, Kyungsu Kim, Sungjin Kim, and Junmo Kim. Learning not to

- learn: Training deep neural networks with biased data. In *Proceedings of the IEEE/CVF Conference on Computer Vision and Pattern Recognition*, pages 9012–9020, 2019. [2](#), [3](#), [15](#)
- [20] Younghyun Kim, Sangwoo Mo, Minkyu Kim, Kyungmin Lee, Jaeho Lee, and Jinwoo Shin. Discovering and mitigating visual biases through keyword explanation. In *Proceedings of the IEEE/CVF Conference on Computer Vision and Pattern Recognition*, pages 11082–11092, 2024. [3](#)
- [21] Ranjay Krishna, Yuke Zhu, Oliver Groth, Justin Johnson, Kenji Hata, Joshua Kravitz, Stephanie Chen, Yannis Kalantidis, Li-Jia Li, David A Shamma, et al. Visual genome: Connecting language and vision using crowdsourced dense image annotations. *International journal of computer vision*, 123:32–73, 2017. [1](#)
- [22] Haoxuan Li, Chunyuan Zheng, Sihao Ding, Peng Wu, Zhi Geng, Fuli Feng, and Xiangnan He. Be aware of the neighborhood effect: Modeling selection bias under interference for recommendation. In *The Twelfth International Conference on Learning Representations*, 2024. [1](#)
- [23] Zhiheng Li, Anthony Hoogs, and Chenliang Xu. Discover and mitigate unknown biases with debiasing alternate networks. In *European Conference on Computer Vision*, pages 270–288. Springer, 2022. [6](#), [7](#), [15](#)
- [24] Zhiheng Li, Ivan Evtimov, Albert Gordo, Caner Hazirbas, Tal Hassner, Cristian Canton Ferrer, Chenliang Xu, and Mark Ibrahim. A whac-a-mole dilemma: Shortcuts come in multiples where mitigating one amplifies others. In *Proceedings of the IEEE/CVF Conference on Computer Vision and Pattern Recognition*, pages 20071–20082, 2023. [3](#), [5](#), [7](#), [13](#), [15](#)
- [25] Tsung-Yi Lin, Michael Maire, Serge Belongie, James Hays, Pietro Perona, Deva Ramanan, Piotr Dollár, and C Lawrence Zitnick. Microsoft coco: Common objects in context. In *Computer Vision—ECCV 2014: 13th European Conference, Zurich, Switzerland, September 6–12, 2014, Proceedings, Part V 13*, pages 740–755. Springer, 2014. [1](#)
- [26] Evan Z Liu, Behzad Haghgo, Annie S Chen, Aditi Raghunathan, Pang Wei Koh, Shiori Sagawa, Percy Liang, and Chelsea Finn. Just train twice: Improving group robustness without training group information. In *International Conference on Machine Learning*, pages 6781–6792. PMLR, 2021. [6](#), [7](#), [15](#)
- [27] Yan Liu, Yu Liu, Xiaokang Chen, Pin-Yu Chen, Daoguang Zan, Min-Yen Kan, and Tsung-Yi Ho. The devil is in the neurons: Interpreting and mitigating social biases in language models. In *The Twelfth International Conference on Learning Representations*, 2024. [1](#)
- [28] Shenyu Lu, Yipei Wang, and Xiaoqian Wang. Debiasing attention mechanism in transformer without demographics. In *The Twelfth International Conference on Learning Representations*, 2024. [2](#)
- [29] Ninareh Mehrabi, Fred Morstatter, Nripsuta Saxena, Kristina Lerman, and Aram Galstyan. A survey on bias and fairness in machine learning. *ACM computing surveys (CSUR)*, 54(6):1–35, 2021. [1](#)
- [30] Valentyn Melnychuk, Dennis Frauen, and Stefan Feuerriegel. Bounds on representation-induced confounding bias for treatment effect estimation. In *The Twelfth International Conference on Learning Representations*, 2024. [1](#)
- [31] Junhyun Nam, Hyuntak Cha, Sungsoo Ahn, Jaeho Lee, and Jinwoo Shin. Learning from failure: De-biasing classifier from biased classifier. *Advances in Neural Information Processing Systems*, 33:20673–20684, 2020. [2](#), [3](#), [6](#), [7](#), [15](#)
- [32] Eirini Ntoutsi, Pavlos Fafalios, Ujwal Gadiraju, Vasileios Iosifidis, Wolfgang Nejdl, Maria-Esther Vidal, Salvatore Ruggieri, Franco Turini, Symeon Papadopoulos, Emmanouil Krasnakis, et al. Bias in data-driven artificial intelligence systems—an introductory survey. *Wiley Interdisciplinary Reviews: Data Mining and Knowledge Discovery*, 10(3):e1356, 2020. [1](#)
- [33] OpenAI. Chatgpt-4, 2023. [Large language model]. [8](#), [13](#)
- [34] Mohammad Pezeshki, Oumar Kaba, Yoshua Bengio, Aaron C Courville, Doina Precup, and Guillaume Lajoie. Gradient starvation: A learning proclivity in neural networks. *Advances in Neural Information Processing Systems*, 34:1256–1272, 2021. [4](#), [7](#)
- [35] Shikai Qiu, Andres Potapczynski, Pavel Izmailov, and Andrew Gordon Wilson. Simple and fast group robustness by automatic feature reweighting. In *International Conference on Machine Learning*, pages 28448–28467. PMLR, 2023. [3](#), [15](#)
- [36] Alec Radford, Jong Wook Kim, Chris Hallacy, Aditya Ramesh, Gabriel Goh, Sandhini Agarwal, Girish Sastry, Amanda Askell, Pamela Mishkin, Jack Clark, Gretchen Krueger, and Ilya Sutskever. Learning transferable visual models from natural language supervision. In *Proceedings of the 38th*

- International Conference on Machine Learning*, pages 8748–8763, 2021. 8, 13
- [37] Shiori Sagawa, Pang Wei Koh, Tatsunori B Hashimoto, and Percy Liang. Distributionally robust neural networks for group shifts: On the importance of regularization for worst-case generalization. *arXiv preprint arXiv:1911.08731*, 2019. 1, 3, 5, 13, 15
  - [38] Ioannis Sarridis, Christos Koutlis, Symeon Papadopoulos, and Christos Diou. Towards fair face verification: An in-depth analysis of demographic biases. In *Proceedings of the International Workshops of ECML PKDD*, 2023. 1
  - [39] Ioannis Sarridis, Christos Koutlis, Symeon Papadopoulos, and Christos Diou. Flac: Fairness-aware representation learning by suppressing attribute-class associations. *IEEE Transactions on Pattern Analysis and Machine Intelligence*, 2024. 2, 3, 6, 13, 15
  - [40] Ioannis Sarridis, Christos Koutlis, Symeon Papadopoulos, and Christos Diou. Badd: Bias mitigation through bias addition. *arXiv preprint arXiv:2408.11439*, 2024. 3, 13, 15
  - [41] Ioannis Sarridis, Christos Koutlis, Symeon Papadopoulos, and Christos Diou. Facex: Understanding face attribute classifiers through summary model explanations. In *Proceedings of the 2024 International Conference on Multimedia Retrieval*, pages 758–766, 2024. 1
  - [42] Enzo Tartaglione, Carlo Alberto Barbano, and Marco Grangetto. End: Entangling and disentangling deep representations for bias correction. In *Proceedings of the IEEE/CVF conference on computer vision and pattern recognition*, pages 13508–13517, 2021. 2, 3, 15
  - [43] Gemma Team, Morgane Riviere, Shreya Pathak, Pier Giuseppe Sessa, Cassidy Hardin, Surya Bhupatiraju, Léonard Hussenot, Thomas Mesnard, Bobak Shahriari, Alexandre Ramé, et al. Gemma 2: Improving open language models at a practical size. *arXiv preprint arXiv:2408.00118*, 2024. 8
  - [44] Angelina Wang, Alexander Liu, Ryan Zhang, Anat Kleiman, Leslie Kim, Dora Zhao, Iroha Shirai, Arvind Narayanan, and Olga Russakovsky. Revise: A tool for measuring and mitigating bias in visual datasets. *International Journal of Computer Vision*, 130(7):1790–1810, 2022. 1
  - [45] Zeyu Wang, Klint Qinami, Ioannis Christos Karakozis, Kyle Genova, Prem Nair, Kenji Hata, and Olga Russakovsky. Towards fairness in visual recognition: Effective strategies for bias mitigation. In *Proceedings of the IEEE/CVF conference on computer vision and pattern recognition*, pages 8919–8928, 2020. 2, 3, 15
  - [46] Shirley Wu, Mert Yuksekgonul, Linjun Zhang, and James Zou. Discover and cure: Concept-aware mitigation of spurious correlation. In *International Conference on Machine Learning*, pages 37765–37786. PMLR, 2023. 3, 6, 15
  - [47] Kai Yuanqing Xiao, Logan Engstrom, Andrew Ilyas, and Aleksander Madry. Noise or signal: The role of image backgrounds in object recognition. In *International Conference on Learning Representations*, 2021. 5
  - [48] Xiaohua Zhai, Basil Mustafa, Alexander Kolesnikov, and Lucas Beyer. Sigmoid loss for language image pre-training. In *Proceedings of the IEEE/CVF International Conference on Computer Vision*, pages 11975–11986, 2023. 8
  - [49] Youcai Zhang, Xinyu Huang, Jinyu Ma, Zhaoyang Li, Zhaochuan Luo, Yanchun Xie, Yuzhuo Qin, Tong Luo, Yaqian Li, Shilong Liu, et al. Recognize anything: A strong image tagging model. In *Proceedings of the IEEE/CVF Conference on Computer Vision and Pattern Recognition*, pages 1724–1732, 2024. 13
  - [50] Zaiying Zhao, Soichiro Kumano, and Toshihiko Yamasaki. Language-guided detection and mitigation of unknown dataset bias. *arXiv preprint arXiv:2406.02889*, 2024. 3

## A. Appendix

### A.1. Theoretical Justification

#### A.1.1. Impact on Gradients

Let us consider a bias-aligned  $\mathbf{x}^{(a)}$  and a bias-conflicting sample  $\mathbf{x}^{(c)}$  with targets  $y^{(a)} = y^{(c)} = \kappa$ . The logits produced by  $f_\theta$  and  $g_\phi$  for each class  $k \in \mathcal{Y}$ , are then  $\mathbf{z}_{\text{main}}^{(a)}(k)$ ,  $\mathbf{z}_{\text{main}}^{(c)}(k)$ ,  $\mathbf{z}_{\text{tag}}^{(a)}(k)$ , and  $\mathbf{z}_{\text{tag}}^{(c)}(k)$ , respectively.  $g_\phi$  encodes visual bias, being irrelevant to class  $\kappa$ , thus we expect  $\mathbf{z}_{\text{tag}}^{(a)}(\kappa) \gg \mathbf{z}_{\text{tag}}^{(c)}(\kappa)$ . Also, bias-aligned samples that contain shortcuts are easier to learn by  $f_\theta$  and therefore it is expected that  $\mathbf{z}_{\text{main}}^{(a)}(\kappa) \geq \mathbf{z}_{\text{main}}^{(c)}(\kappa)$ . These imply:

$$\begin{aligned} \mathbf{z}_{\text{main}}^{(a)}(\kappa) + \mathbf{z}_{\text{tag}}^{(a)}(\kappa) &\gg \mathbf{z}_{\text{main}}^{(c)}(\kappa) + \mathbf{z}_{\text{tag}}^{(c)}(\kappa) \Rightarrow \\ \sigma^{(\kappa)}(\mathbf{z}_{\text{main}}^{(a)} + \mathbf{z}_{\text{tag}}^{(a)}) &\gg \sigma^{(\kappa)}(\mathbf{z}_{\text{main}}^{(c)} + \mathbf{z}_{\text{tag}}^{(c)}) \Rightarrow \\ \frac{1}{\sigma^{(\kappa)}(\mathbf{z}_{\text{main}}^{(a)} + \mathbf{z}_{\text{tag}}^{(a)})} &\ll \frac{1}{\sigma^{(\kappa)}(\mathbf{z}_{\text{main}}^{(c)} + \mathbf{z}_{\text{tag}}^{(c)})} \end{aligned} \quad (4)$$

where  $\sigma^{(k)}$  denotes the  $k$ th class' softmax score.

Additionally,  $f_\theta$  after a few iterations learns bias-aligned samples (based either on relevant or irrelevant class features) indicating  $\arg \max_{k \in \mathcal{Y}} \mathbf{z}_{\text{main}}^{(a)}(k) = \kappa$ , while  $\arg \max_{k \in \mathcal{Y}} \mathbf{z}_{\text{tag}}^{(a)}(k) = \kappa$ , by definition. Hence,  $\sigma^{(\kappa)}(\mathbf{z}_{\text{main}}^{(a)} + \mathbf{z}_{\text{tag}}^{(a)}) \approx 1$  leading to diminished gradients  $\frac{\partial}{\partial \theta_0} [\sigma^{(\kappa)}(\mathbf{z}_{\text{main}}^{(a)} + \mathbf{z}_{\text{tag}}^{(a)})] \approx 0$ . On the other hand,  $\sigma^{(\kappa)}(\mathbf{z}_{\text{main}}^{(c)} + \mathbf{z}_{\text{tag}}^{(c)}) \in (0, 1)$  leading to gradients  $\frac{\partial}{\partial \theta_0} [\sigma^{(\kappa)}(\mathbf{z}_{\text{main}}^{(c)} + \mathbf{z}_{\text{tag}}^{(c)})] > 0$ . Hence:

$$\frac{\partial}{\partial \theta_0} [\sigma^{(\kappa)}(\mathbf{z}_{\text{main}}^{(a)} + \mathbf{z}_{\text{tag}}^{(a)})] \leq \frac{\partial}{\partial \theta_0} [\sigma^{(\kappa)}(\mathbf{z}_{\text{main}}^{(c)} + \mathbf{z}_{\text{tag}}^{(c)})] \quad (5)$$

Combining Eq. (4) and Eq. (5) we get:

$$\begin{aligned} \frac{1}{\sigma^{(\kappa)}(\mathbf{z}_{\text{main}}^{(a)} + \mathbf{z}_{\text{tag}}^{(a)})} \cdot \frac{\partial}{\partial \theta_0} [\sigma^{(\kappa)}(\mathbf{z}_{\text{main}}^{(a)} + \mathbf{z}_{\text{tag}}^{(a)})] &\ll \\ \frac{1}{\sigma^{(\kappa)}(\mathbf{z}_{\text{main}}^{(c)} + \mathbf{z}_{\text{tag}}^{(c)})} \cdot \frac{\partial}{\partial \theta_0} [\sigma^{(\kappa)}(\mathbf{z}_{\text{main}}^{(c)} + \mathbf{z}_{\text{tag}}^{(c)})] &\Rightarrow \\ \frac{\partial}{\partial \theta_0} [\log \sigma^{(\kappa)}(\mathbf{z}_{\text{main}}^{(a)} + \mathbf{z}_{\text{tag}}^{(a)})] &\ll \\ \frac{\partial}{\partial \theta_0} [\log \sigma^{(\kappa)}(\mathbf{z}_{\text{main}}^{(c)} + \mathbf{z}_{\text{tag}}^{(c)})] &\Rightarrow \\ \frac{\partial}{\partial \theta_0} \left[ \sum_k \mathbb{1}(a, k) \cdot \log \sigma^{(k)}(\mathbf{z}_{\text{main}}^{(a)} + \mathbf{z}_{\text{tag}}^{(a)}) \right] &\ll \\ \frac{\partial}{\partial \theta_0} \left[ \sum_k \mathbb{1}(c, k) \cdot \log \sigma^{(k)}(\mathbf{z}_{\text{main}}^{(c)} + \mathbf{z}_{\text{tag}}^{(c)}) \right] &\Rightarrow \\ \frac{\partial \mathcal{L}^{cls}(\mathbf{x}^{(a)})}{\partial \theta_0} &\ll \frac{\partial \mathcal{L}^{cls}(\mathbf{x}^{(c)})}{\partial \theta_0} \end{aligned} \quad (6)$$

where

$$\mathbb{1}(i, k) = \begin{cases} 1 & \text{if } y_i = k \\ 0 & \text{otherwise} \end{cases} \quad (7)$$

which indicates that through our framework the main model  $f_\theta$  is enforced to update its weights based mainly on the gradients corresponding to the bias-conflicting samples  $\mathbf{x}^{(c)}$ . This essentially means that  $f_\theta$  will eventually ignore the visual cues prevalent in  $\mathbf{x}^{(a)}$  samples corresponding to irrelevant information encoded by the tag model  $g_\phi$ .

#### A.1.2. Unbiased Distribution Learning

Let  $p_{tr}(X, Y, B)$  be the training data distribution where  $X$ ,  $Y$ ,  $B$  are random variables associated with the data, the label and the bias attribute, respectively. From Theorem 1 of [16] we know that if  $P_u$  is a shift of  $p_{tr}$  such that the distribution  $P_u(Y|B)$  is uniform (and therefore unbiased), then for a model  $f_\theta = p_u(y|\mathbf{x})$  that estimates the conditional probability over  $P_u$ , its probability over  $p_{tr}$  will be

$$p_{tr}(y|\mathbf{x}) = \frac{\exp(\mathbf{z}_{\text{main}}(y) + \log p_{tr}(y|b))}{\sum_{y'} \exp(\mathbf{z}_{\text{main}}(y') + \log p_{tr}(y'|b))} \quad (8)$$

In the case of MAVias, let the probability  $p_{tr}(y|b)$  be estimated through the projection and

classification layers,  $\mathbf{z}_{\text{tag}} = f_{\theta_c}(g_\phi(\mathbf{e}))$  which use the visual bias embeddings  $\mathbf{e}$  (encoding the irrelevant tags) to produce logits  $\mathbf{z}_{\text{tag}}$ . As a result,

$$\begin{aligned} \log p_{tr}(y|b) &= \log \frac{e^{\mathbf{z}_{\text{tag}}(y)}}{\sum_{y''} e^{\mathbf{z}_{\text{tag}}(y'')}} \\ &= \mathbf{z}_{\text{tag}}(y) - \log \left( \sum_{y''} e^{\mathbf{z}_{\text{tag}}(y'')} \right) \quad (9) \\ &= \mathbf{z}_{\text{tag}}(y) - A(\mathbf{z}_{\text{tag}}) \end{aligned}$$

where  $A(\mathbf{z}_{\text{tag}}) = \sum_{y''} e^{\mathbf{z}_{\text{tag}}(y'')}$ . Replacing Eq. (9) to Eq. (8) gives

$$\begin{aligned} p_{tr}(y|\mathbf{x}) &= \\ &= \frac{\exp(\mathbf{z}_{\text{main}}(y) + \mathbf{z}_{\text{tag}}(y) - A(\mathbf{z}_{\text{tag}}))}{\sum_{y'} \exp(\mathbf{z}_{\text{main}}(y') + \mathbf{z}_{\text{tag}}(y') - A(\mathbf{z}_{\text{tag}}))} \\ &= \frac{\exp(-A(\mathbf{z}_{\text{tag}})) \exp(\mathbf{z}_{\text{main}}(y) + \mathbf{z}_{\text{tag}}(y))}{\exp(-A(\mathbf{z}_{\text{tag}})) \sum_{y'} \exp(\mathbf{z}_{\text{main}}(y') + \mathbf{z}_{\text{tag}}(y'))} \\ &= \frac{e^{(\mathbf{z}_{\text{main}}(y) + \mathbf{z}_{\text{tag}}(y))}}{\sum_{y'} e^{(\mathbf{z}_{\text{main}}(y') + \mathbf{z}_{\text{tag}}(y'))}} \quad (10) \end{aligned}$$

thus leading to the logit addition of Eq. (2).

For this approach to work, however, one must ensure that models  $g_\phi$  and  $f_{\theta_c}$  are successfully trained to produce logits  $\mathbf{z}_{\text{tag}}$  that predict  $p_{tr}(y|b)$  and are not dominated by  $\mathbf{z}_{\text{main}}$ . This is achieved by the regularization term of Eq. (3) which controls the magnitude differences of  $\mathbf{z}_{\text{main}}$  and  $\mathbf{z}_{\text{tag}}$ .

## A.2. Experimental Setup

### A.2.1. Model architectures

For comparability purposes, we employ the same network architectures as those used in other works [2, 16, 39, 40]. In particular, for CelebA, we adopt the ResNet-18 architecture [14], for Waterbirds, UrbanCars, and ImageNet9 datasets we use Resnet-50 networks. In all experiments, the projection layer is a dense layer that gets vision-language embeddings as input and its output size is aligned to the feature size of the main model.

### A.2.2. Implementation details

The SGD optimizer is employed for all datasets except for CelebA, where Adam optimizer is used.

We use an initial learning rate of 0.001, which is divided by 10 every 1/3 of the training epochs. The weight decay is set to  $10^{-4}$ . The batch size is 128 for CelebA and 64 for Waterbirds, UrbanCars, and ImageNet9. Following previous works [16, 24, 37], we train the models for 40, 100, 300, and 40 for CelebA, Waterbirds, UrbanCars, and ImageNet9, respectively. For Waterbirds and UrbanCars, we do not use a learning rate scheduler. The parameters  $(\alpha, \lambda)$  are (0.01, 0.5), (0.05, 0.6), (0.01, 0.4), and (0.001, 0.7) for CelebA, Waterbirds, UrbanCars, and ImageNet9, respectively. The optimal values of the hyperparameters are derived through a grid search. RAM [49], ChatGPT-4o [33], CLIP [36] are employed for image tagging, irrelevant tag filtering, and vision-language encoding, respectively. Experiments on CelebA, Waterbirds, and UrbanCars, were conducted on an NVIDIA A100 GPU, while experiments on Imagenet were conducted on a single NVIDIA RTX-4090 GPU. All experiments were repeated for 5 different random seeds.

### A.2.3. Prompting

To ensure accurate tag classification, we provide the LLM with a detailed system prompt. Tags are processed in batches of 100, as testing has shown that longer lists can lead to some tags being overlooked. Since relevant tags are significantly fewer than irrelevant ones, we instruct the LLM to return only the relevant tags, allowing us to deduce the irrelevant ones. The exact system prompt is presented in Fig. 5

## A.3. Two-moon Distribution Experiment

To demonstrate the capability of MAVias in mitigating biased features, we extend the classic two-moon distribution into a 3-dimensional setting. In this scenario, we consider a dataset  $\mathcal{D} = \{(\mathbf{x}^{(i)}, y^{(i)})\}_{i=1}^N$ , where each input  $\mathbf{x}^{(i)} = (x_1^{(i)}, x_2^{(i)}, x_3^{(i)})$  consists of two relevant features  $x_1^{(i)}, x_2^{(i)}$  and an additional irrelevant feature  $x_3^{(i)}$  that introduces bias. The target label  $y^{(i)}$  should be determined based on the features  $x_1^{(i)}, x_2^{(i)}$ , following the typical two-moon structure, while the feature  $x_3^{(i)}$  represents the bias (e.g., samples are linearly separable with respect to  $x_3^{(i)}$ , even though



### System Prompt

I will provide you with the name of a target class and a large list of tags. Your task is to evaluate the tags and identify only those directly related to the target class. A tag is considered relevant if it describes or is an essential part of the object associated with the class name. This includes tags that refer to: physical components, defining features, inherent characteristics, and essential behaviors or functions of the object. For example, if the target class is “bee” tags like “insect”, “wing”, and “buzz” are relevant because they describe core aspects of what a bee is or does.

Conversely, a tag is irrelevant if it refers to elements that are not an intrinsic part of the object. Irrelevant tags may include: background details, environmental context, colors (unless a defining characteristic), lighting, textures, other objects, or other non-essential contextual elements.

For example, in the case of the class “bee”, tags like “sky”, “flower”, or “blue” would be irrelevant, as they describe the environment or background rather than the bee itself.

Please output only the relevant tags in JSON format only (i.e., `{ relevant_tags: [the list of tags]}`).

Figure 5. LLM system prompt for deriving the relevant tags.

it should not be used for classification).

In this setup, the main model  $f_{\theta}(\mathbf{x}^{(i)})$  receives the full input  $\mathbf{x}^{(i)} = (x_1^{(i)}, x_2^{(i)}, x_3^{(i)})$ , while the projection layer  $g_{\phi}(x_3^{(i)})$  is provided only with the irrelevant feature  $x_3^{(i)}$ . The projection layer helps the system to explicitly account for this bias by incorporating  $x_3^{(i)}$  in a controlled manner, while the main model is encouraged to focus on the relevant features  $x_1^{(i)}$  and  $x_2^{(i)}$  for classification. As shown in

Fig. 6, MAVias enables the main model to effectively learn the underlying two-moon distribution based on the features  $x_1^{(i)}, x_2^{(i)}$ , while the vanilla model relies only on the biased feature  $x_3^{(i)}$ , treating it as a shortcut that prevents the model from learning the proper distribution.

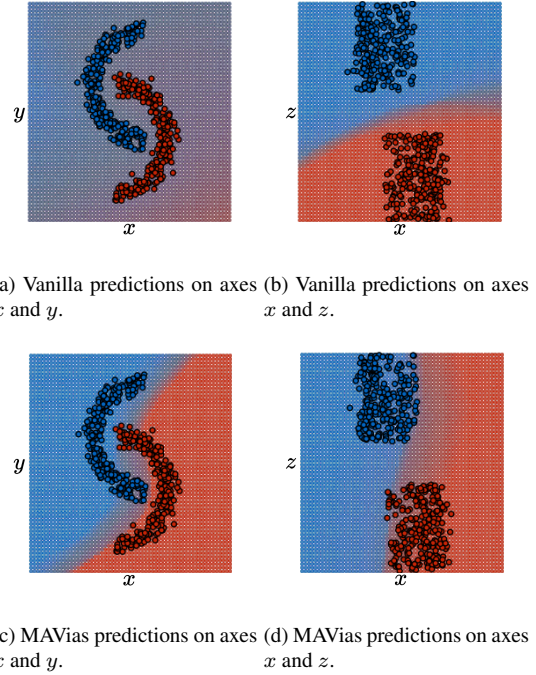


Figure 6. Two-moon problem on 3 dimensions. The distributions are linearly separable on axis  $z$  (i.e.,  $z$  feature introduces bias), while the actual target is to learn the distributions defined by the features  $x$  and  $y$ .

### A.4. Comparative Analysis

This section provides a comprehensive comparative analysis involving both bias label-aware (BA) and bias label-unaware (BU) methodologies. As shown in Tab. 10, MAVias demonstrates competitive performance on CelebA compared to the best-performing BA method, i.e., -0.6% bias-conflict accuracy and -1.5% unbiased accuracy, even though MAVias has no access to bias-related information. Furthermore, Tab. 11 evaluates MAVias on Waterbirds, a well-known benchmark for spuri-

Table 10. Evaluation of the proposed method on CelebA with *BlondHair* and *gender* as biased attribute and target, respectively. Bold denotes the best-performing bias label-unaware (BU) method and underlined denotes the best-performing bias label-aware method.

Methods	BU	Bias	
		BlondHair	
		Unbiased	Bias-conflict
LNL [19]	✗	80.1±0.8	61.2±1.5
DI [45]	✗	90.9±0.3	86.3±0.4
EnD [42]	✗	86.9±1.0	76.4±1.9
BC-BB [16]	✗	<u>91.4±0.0</u>	87.2±0.2
FairKL [2]	✗	81.7±1.7	69.9±2.4
FLAC [39]	✗	91.2±0.3	<u>88.7±0.5</u>
LfF [31]	✓	84.2±0.3	81.2±1.4
SoftCon [16]	✓	84.1	74.4
FLAC-B [39]	✓	87.0±0.6	84.9±2.2
MAVias	✓	<b>89.7±0.6</b>	<b>87.1±1.7</b>

Table 11. Evaluation on Waterbirds.

Method	BU	WG Acc.	Avg. Acc.
GroupDro [37]	✗	90.6±1.1	91.8±0.3
BAdd [40]	✗	92.9±0.3	93.6±0.2
DFR [35]	✗	<u>92.9±0.2</u>	<u>94.2±0.4</u>
JTT [26]	✓	86.7±1.5	93.3±0.3
DISC [46]	✓	88.7±0.4	93.8±0.7
MAVias	✓	<b>93.7±0.4</b>	<b>94.5±0.4</b>

ous correlation problems between bird type and background environment. Notably, MAVias attains 93.7% Worst-Group accuracy, outperforming all compared BA methods, i.e., GroupDRO, BAdd, and DFR. Also, MAVias achieves this improvement while maintaining competitive average accuracy (+0.3%), which indicates that the reduction in bias did not come at the cost of overall performance. In contrast, BU methods like JTT and DISC, which can be directly compared with MAVias, show a larger gap in WG performance, indicating their limited effectiveness as a result of the lack of bias information (i.e., type of bias or bias labels), a limitation that MAVias successfully addresses.

Finally, Tab. 12 presents the performance of

Table 12. Evaluation on UrbanCars.

Method	BU	I.D. Acc	BG Gap	CoObj Gap	BG+CoObj Gap
GroupDro [37]	✗	91.6	-10.9	-3.6	-16.4
DFR [35]	✗	89.7	-10.7	-6.9	-45.2
LLE [24]	✗	96.7	<u>-2.1</u>	-2.7	-5.9
BAdd [40]	✗	91.0±0.7	-4.3±0.4	<u>-1.6±1.0</u>	<u>-3.9±0.4</u>
LfF [31]	✓	97.2	-11.6	-18.4	-63.2
JTT [26]	✓	95.9	-8.1	-13.3	-40.1
Debian [23]	✓	98.0	-14.9	-10.5	-69.0
MAVias	✓	92.8±0.8	<b>-4.1±0.6</b>	<b>-2.4±1.4</b>	<b>-6.7±1.4</b>

Table 13. MAVias:  $g_\theta(\cdot)$  accuracy for the UrbanCars training samples belonging to subgroups of *urban car* class with different biases.

BG	CoObj	#samples	$g_\theta(\cdot)$ acc.
Country	Country	10	00.00
Country	Urban	190	54.21
Urban	Country	190	67.36
Urban	Urban	3610	98.42

the relevant methods on the UrbanCars dataset. This benchmark poses a greater challenge due to the presence of multiple biases, as reflected in the results, i.e., most BU methods perform significantly worse than BA methods. However, MAVias achieves competitive performance, with only 2%, 0.8%, and 2.8% drops in BG, CoObj, and BG+CoObj Gaps, respectively, compared to the best-performing BA methods.

## A.5. Ablation Study

First, let us report the accuracy of  $g_\phi(\cdot)$  on the training samples of the *urban car* class from the UrbanCars dataset, which correlates the target classes with relevant backgrounds and co-occurring objects. As shown in Tab. 13, the  $g_\phi$  shows a clear distinction in its performance: its accuracy increases from 0% for bias-conflicting samples (i.e., those with a *country* background and co-occurring object) to 98.42% for bias-aligned samples (i.e., those with an *urban* background and co-occurring object). This result confirms that our tag-based approach produces embeddings that effectively capture bias, providing a foundation for the main model  $f_\theta(\cdot)$  to focus on learning unbiased features.

Furthermore, we investigate the impact of the vocabulary size employed for image tagging. The

Table 14. Performance of MAVias across varying portions of the original tag vocabulary. Results pertain to the Waterbirds dataset.

size	WG Acc.	Avg. Acc.
10%	78.1	87.1
20%	79.4	89.0
30%	91.1	92.0
40%	93.1	92.3
50%	93.8	93.2
60%	93.2	93.5
70%	92.9	94.2
80%	93.0	94.3
90%	93.6	94.5
100%	93.7	94.5

Table 15. Comparison of MAVias performance on Waterbirds using different approaches for computing embeddings from tags. “Separately” denotes computing individual embeddings for each tag and then averaging them, while “collectively” denotes computing a single embedding for all tags combined.

Type	WG Acc.	Avg. Acc.
separately	$93.0 \pm 0.2$	$93.6 \pm 0.2$
collectively	$93.7 \pm 0.4$	$94.5 \pm 0.4$

original vocabulary RAM uses has a size of 4585 words. Tab. 14 reports the performance of MAVias for different portions of the original vocabulary. Notably, using 30% or more of the original vocabulary yields highly effective models, which is due to the dataset’s bias (aquatic or terrestrial environments) that a variety of tags can capture.

Moreover, Tab. 15 reports the performance of MAVias when computing individual embeddings for each tag and then averaging them compared to the one computing a single embedding for all tags combined. As one may observe, although both are highly effective, the latter can provide more representative features.

Finally, Fig. 7 illustrates the impact of different values of hyperparameters  $\alpha$  and  $\lambda$  on the MAVias performance.

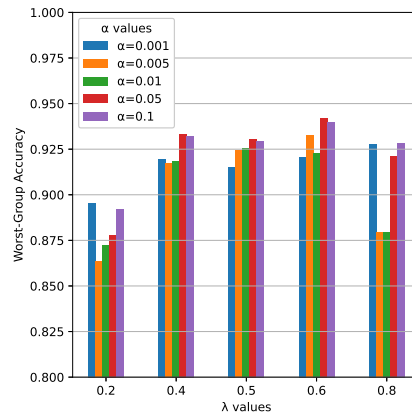


Figure 7. Impact of hyperparameters  $\alpha$  and  $\lambda$  on the Worst-Group accuracy on the Waterbirds dataset.